Progress in Natural Science: Materials International 26 (2016) 510–515

HOSTED BY

Contents lists available at ScienceDirect

Progress in Natural Science: Materials International

journal homepage: www.elsevier.com/locate/pnsmi

Letter

Ligand effects on the structure and vibrational properties of the thiolated Au_{18} cluster

Alfredo Tlahuice-Flores

CICFIM-Facultad de Ciencias Físico-Matemáticas, Universidad Autónoma de Nuevo León, San Nicolás de los Garza, NL 66450, Mexico

ARTICLE INFO

Keywords:
Gold cluster
Ligand effects
Structure
Vibration
$Au_{18}(SR)_{14}$
Density functional theory

ABSTRACT

Most of the studies devoted to thiolated gold clusters suppose that their core and Au-S framework do not suffer from distortion independently of the protecting ligands (-SR) and it is assumed as correct to simplify the ligand as SCH_3. In this work is delivered a systematic study of the structure and vibrational properties (IR and Raman) of the $Au_{18}(SR)_{14}$ cluster. The pursued goal is to understand the dependency of the displayed vibrational properties of the thiolated Au_{18} cluster with the ligands type. A set of six ligands was considered during calculations of the vibrational properties based on density functional theory (DFT) and in its dispersion-corrected approach (DFT-D).

1. Introduction

The identification of new compounds is essential in novel fields of nanotechnology and in the case of thiolated gold clusters [1], in 2007 it was possible to obtain a sight of the core and Au-S framework of the $Au_{102}(SR)_{44}$ cluster [2]. The structure of this new type of compounds is comprised by a central gold core protected by Au_nS_{n+1} units called staple motifs [3]. The inner core can hold symmetry as in the anionic $Au_{25}(SR)_{18}$ cluster [4] which holds a C_i point group [5], or it can be no symmetric as in $Au_{18}(SR)_{14}$ cluster (C_1 symmetry) [6]. The number of Au atoms constituting the central core varies but one tetrahedral Au_4 core has been determined as the smallest core constituting the $Au_{15}(SR)_{13}$ cluster [7]. The importance of these compounds is due to their interesting size-depending properties and to their potential applications in catalysis, bio-sensing and nanomedicine [8].

The presence of certain chemical groups can be revealed by their corresponding bands both in the Infrared and Raman spectra, and assisted by theoretical calculations during the assignment of featured bands. However, as those calculations are based on the harmonic approximation, is necessary to use a scaling factor in order to take into account the anharmonic effects. This approach allows to match calculations with the experiment. Experimentally, IR spectroscopy has been used for this kind of compounds previously [9–13]. On the theoretical side, worthy of note is the work by Tlahuice-Flores in 2013, where it was reported that it is possible to distinguish between anionic compounds such as monometallics $Au_{25}(SCH_3)_{18}$, and $Ag_{25}(SCH_3)_{18}$ and one alloy of silver and gold atoms ($Ag_{12}Au_{13}(SCH_3)_{18}$) by means of their infrared spectra [14]. In this work, the key was to compare both CH_3 umbrella and C-S stretching modes (frequency values). In a more general study, it was proposed that vibrational spectra (IR and Raman) can be used as a *fingerprint* to distinguish between various thiolated gold clusters. The study was focused on the low-frequency range (20–350 cm^{-1}) of small thiolated gold clusters where the relevant Au-S modes appears [5]. Guided for mentioned reports, Dolamic et al., carried out an experimental study of the far-IR of Au_{25}, Au_{38}, Au_{40} and Au_{144} clusters protected by 2-phenylethylthiolate (SCH_2CH_2Ph) ligand. They reported subtle differences on the vibrational spectra and a slightly shift in their intensities but no in their frequencies [13]. The mentioned experimental results left open the question regarding the influence of the ligands in the properties of thiolated gold clusters, and the possibility to characterize their structures and therefore to distinguish them.

The influence of the ligands on the structure of thiolated gold clusters was found during the study of a new structural model of the $Au_{15}(SR)_{13}$ cluster. It was stated that by using N-acetyl-L-cysteine (NAC) as ligands, an isomer comprised by one Au_4 core was protected by both one heptamer and one tetramer motifs was obtained [7]. To date the ligand effects [5], on the structure of thiolated gold clusters is reported on the thiolated Au_{24} cluster, were thiolate or selenolate ligands, arrange forming various staple motifs [15]. Furthermore, thiolated Au_{40} cluster is constituted by an oblate Au_{26} core [16], or by a snowflake-like Au_{25} core [17], depending whether a 2-phenylethylthiolate or a 2-methylbenzenethiolate ligand has been used during experiments. On the other hand, the thiolated Au_{36} cluster has been synthetized with three different type of ligands (SPh, SPh-*t*-Bu and SC_5H_9) [18], and unexpectedly the core maintains the same

Peer review under responsibility of Chinese Materials Research Society.
E-mail address: tlahuicef@gmail.com.

http://dx.doi.org/10.1016/j.pnsc.2016.09.008
Received 31 July 2016; Accepted 16 August 2016
Available online 13 October 2016

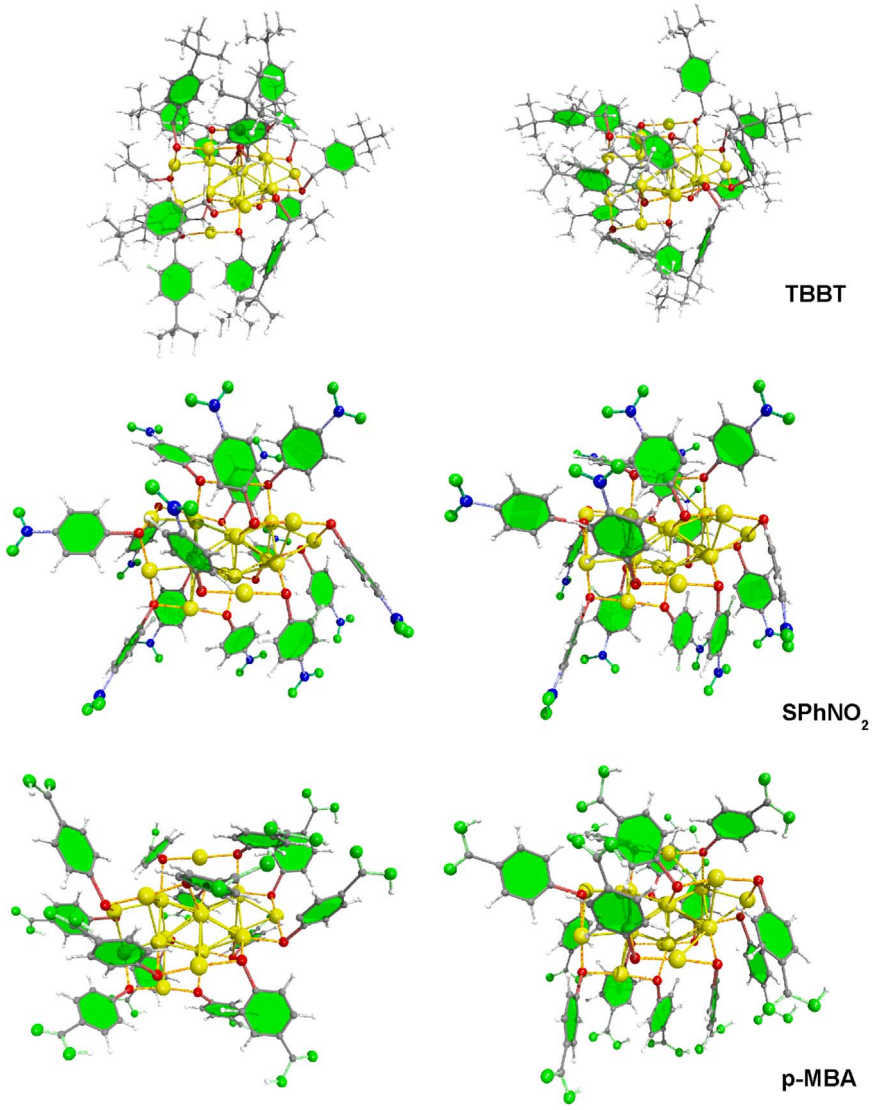

Fig. 1. Optimized Au_{18} clusters protected with three different ligands. Au, S, C, N, O, and H atoms are yellow, red, gray, blue, green, and white, respectively. Clusters relaxed by means of DFT-D are located at right panel. a) Phenyl rings orientate allowing to COOH groups to interact forming ordered patterns, b) Au_{18} Cluster protected by $SPhNO_2$ ligands, displays a major interaction between near NO groups shifting the orientation of phenyl rings, c) When TBBT ligands are protecting the Au_{18} cluster (right panel), phenyl rings show a distinct orientation while the gold core seems to maintain intact.

number of Au atoms. This might be attributed to a strong or stable inner core, which despite the interaction with ligands is kept intact. The influence of the mentioned ligands can be ascribed to their bulkiness (SPh-*t*-Bu or TBBT) or due to its aromaticity (SPh ligand), while SC_5H_9 ligand (nonaromatic) was expected to have a moderate influence in the structural properties [18]. Therefore, to study the effect of various ligands is necessary to determine the interaction either among gold core atoms and ligands or among ligands (interligand interactions) where the consideration of long range interactions is mandatory.

Regarding the structure of the thiolated Au_{18} cluster, it is comprised by one Au_9 core which resembles three alternated Au_3 units and covered with three monomer motifs located around them, while one dimer and one tetramer motifs are located at the endings of the Au_9 core. Moreover, it holds one special Au atom which is linked to three S atoms.

1.1. Theoretical methodology

In this communication, all calculations were carried out based both on DFT and dispersion-corrected density functional theory (DFT-D) which take into account longer-ranged van der Waals interactions, by using the method of Grimme et al. [19,20] The generalized gradient approximation (GGA) [21], and the Perdew–Burke–Ernzerhof (PBE) exchange-correlation functional was used [22]. The LANL2DZ basis set were employed for Au atoms (19 valence electrons) and 6–31 G(d,p) basis set for H, S, C, N, and O atoms. Structural optimizations were performed using a force tolerance criterion of 0.01 eV/Å. The consideration of diffuse functions is mandatory for the correct prediction of infrared intensities [23]. All mentioned methodology is implemented in Gaussian 09 package (G09) [24]. The mentioned DFT methodology has been proved by the author in the study of thiolated gold clusters [5,7,14].

A set of six ligands was selected in order to carry out this study. The set includes p-mercaptobenzoic acid (*p*-MBA) [2], SPh that has been found in thiolated Au_{99} [25], Au_{23} [26], and $Au_{102}(SR)_{44}$ clusters [27], $SPhNO_2$, 4-*tert*-Butylbenzenethiol (TBBT=SPh-*t*-Bu) which have found in various thiolated gold clusters [28–32], cyclohexanethiol (S-*c*-C_6H_{11}) which is the ligand present in the thiolated Au_{64} cluster [33] and into the experimental structure of the thiolated Au_{18} cluster [34]. In addition it was considered the SCH_3 ligand which is amply used during calculations. The justification to study the thiolated Au_{18} cluster is due to its interesting photoluminescence properties [35].

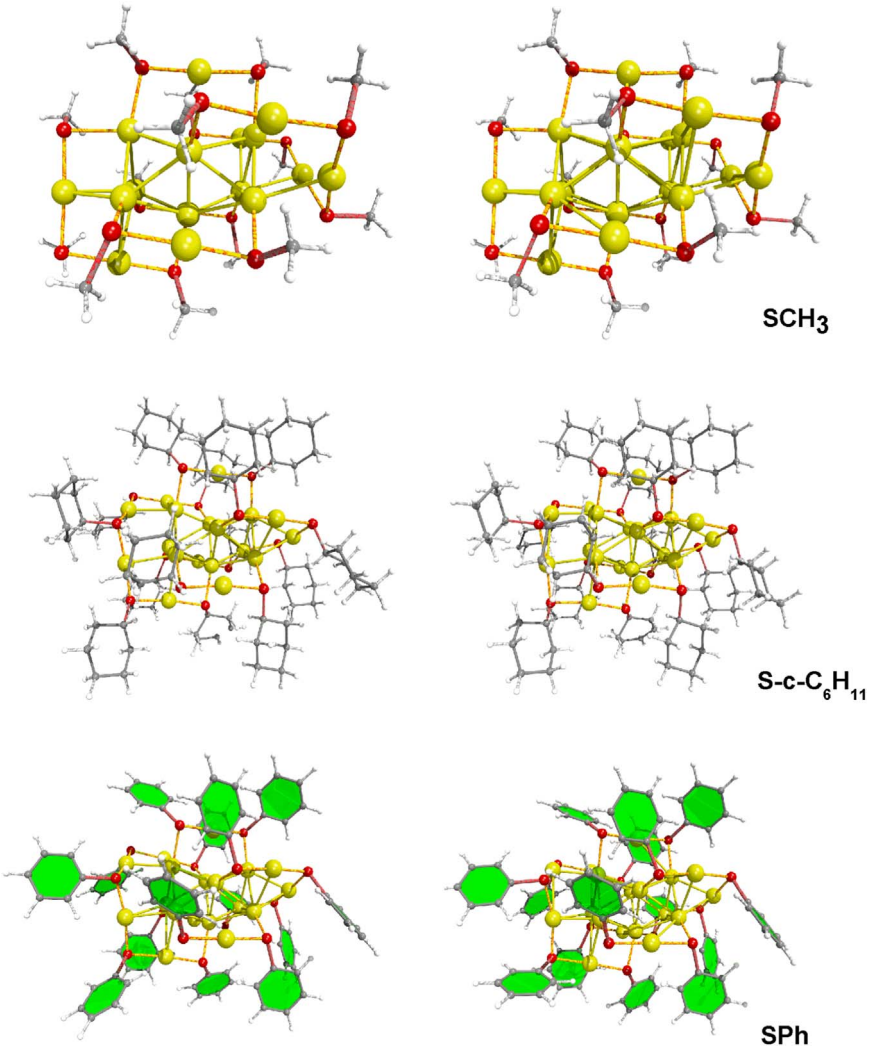

Fig. 2. Structure of the optimized Au_{18} cluster protected with three kinds of ligands. Au, S, C, and H atoms are yellow, red, gray, and white, respectively. a) Au_{18} cluster protected by SPh ligands does not show a clear difference on the orientation of the phenyl rings (depicted in green) after considering the long range interactions (right panel), b) Au_{18} cluster protected with S-c-C_6H_{11} ligands display a similar structure independently of the kind of calculations, c) Au_{18} cluster protected with SCH_3 ligands does not show an influence of the consideration of the long range interactions (right panel), and the core and Au-S framework seems to maintain intact.

2. Results and discussion

Starting from the parent Au_{18} cluster protected by S-*c*-C_6H_{11} ligands, a set of initial structures was built, which is depicted in Figs. 1 and 2. After a relaxation based on a DFT-D approach, it was found a distinct orientation of some ligands with respect to the DFT optimized structures (Fig. 1). However, SPh, S-*c*-C_6H_{11}, and SCH_3 ligands (Fig. 2), shows a similar orientation for both kind of calculations (see Figs. S2-S7). This indicates that the well-known interaction between phenyl rings [36], is diminished in the Au_{18} cluster protected with SPh ligands, and this must be ascribed to the space available on the surface of the gold core, which might reduce the steric hindrance.

A further analysis revealed that even when bulky TBBT ligands are orientated in different manner after considering van der Waals interactions, surprisingly the core is maintained intact being similar to the core of the cluster protected by S-*c*-C_6H_{11} ligands (Fig. 3d). Regarding *p*-MBA ligands, they induce strong distortion into the Au-S framework of the thiolated Au_{18} cluster; this result is in accordance with an early study devoted to the thiolated Au_{25} cluster [5]. Moreover, the DFT-D optimized Au_{18}(p-MBA)$_{14}$ cluster features distinctive Au bond lengths in the inner core (Au_c-Au_c bonds) and between core and staples (Au_c-Aus). The interligand interaction among O-H and C=O groups results in a compact gold core with less dispersed Au_c-Au_c bonds while S-C bond lengths reduce slightly. The borderline between Au-S and Au-Au bonds is indicated by a dotted line in Fig. 3, and a complete comparison of the bonding displayed by DFT and DFT-D structures is organized in Fig. S1. This result demonstrates that the effect of the ligands cannot be ascribed merely to their bulkiness but to the presence of chemical groups and to their interaction.

The presence of an "intact" core despite the presence of SCH_3, SPh, and S-c-C_6H_{11} ligands, supporting the idea of a strong core, where the electronic part is important. Another interesting structural difference displayed by DFT and DFT-D relaxed clusters involves deflections into the tetramer motif (Figs. S2 and S4). Given the structural differences between studied clusters, it was expected that the vibrational properties could be different even in the 20–350 cm^{-1} range where the characteristic Au-Au and Au-S vibrations might appear [5].

Fig. 4 shows a comparison of the calculated IR and Raman spectra based on DFT calculations. In general, p-MBA and $SPhNO_2$ ligands, which induce major structural distortions, shows less intense Raman spectra after including long range interactions (Fig. S8). However, they hold the more intense Raman spectra between all studied structures. Another important feature found in all Raman spectra is a peak located circa 300 cm^{-1} due to the Au-S stretching on the staples coupled with bending modes of C atoms constituting phenyl rings (dotted line of Fig. 4). Conversely, the structures protected with ligands do not induce

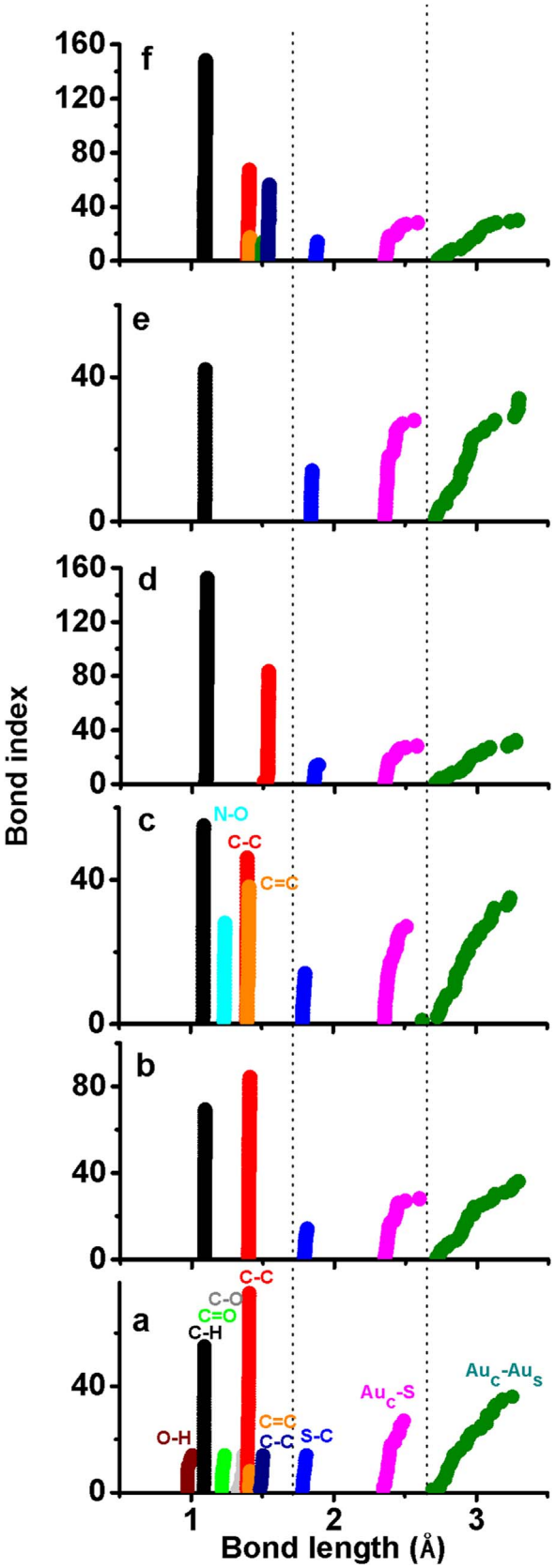

Fig. 3. Bond lengths of relaxed thiolated Au_{18} structures based on DFT-D calculations. Structures are protected by **a** p-MBA, **b** SPh, **c** $SPhNO_2$, **d** cyclohexyl, **e** SCH_3, and **f** TBBT ligands. Coloured labels are used to identify bonds present in each compound. It is found that Au_{18} protected with p-MBA, SPh and $SPhNO_2$ depicts short S-C bonds.

strong distortions into the Au-S framework, showing the similar feature of IR and Raman spectra. For example, SCH_3 ligand results in similar IR and Raman spectra based on either DFT or DFT-D calculations (Fig. S8).

It is straight to inquire how the range comprising the Au-Au and Au-S vibrations is changed due to the effect of ligands. It was found that the upper range of frequencies where Au-Au and Au-S vibrations appear depends on the ligand type; SCH_3 holds a 324.10 cm^{-1} frequency; TBBT presents a 331.50 cm^{-1}; S-*c*-C_6H_{11} shows a value of 377.48 cm^{-1}; *p*-MBA features a frequency of 383.46 cm^{-1}; SPh structure holds a 386.21 cm^{-1} value, and $SPhNO_2$ a 387.68 cm^{-1} frequency. This result was expected because the upper frequency value corresponds primarily with a tangential movement of the S atoms located on staple motifs, but it depends on the attached ligand as well (remember that S-C bonds are short in *p*-MBA protected Au_{18} cluster).

Regarding the IR spectrum displayed by the cluster protected by p-MBA ligands, it is circa two times more intense and shows some similitudes with the cluster including $SPhNO_2$ ligands. However, IR spectra show that the peaks varies in intensity, and it is not easy to find a trend. This suggests that IR spectra might be not adequate to characterize the Au_{18} cluster due to their strong dependency with those ligands used during calculations. Whence, Raman spectra seem more adequate, for example, *p*-MBA and $SPhNO_2$ have similar bands, while SPh, TBBT, and S-c-C_6H_{11} resemble each other. It is important to mention that the spectrum of Au_{18} cluster protected by SCH_3 ligand features a peak circa 300 cm^{-1} as well.

A further analysis of the normal modes displayed by the Au_{18} cluster protected by p-MBA ligands can be summarized as follows. From 6.78 to 17.53 cm^{-1} wagging modes of the phenyl rings was observed. Up to 23.08 cm^{-1} a mixture of wagging and rocking modes of phenyl rings was found. Starting from 24.71 cm^{-1} and up to 55.55 cm^{-1} phenyl rings vibrated following a twisting bending mode. And from 56.79 to 66.00 cm^{-1} S and Au core atoms participated in the bending normal modes. The stretching Au_c-S modes were found from 111.44 cm^{-1}, f) located at 119.34 cm^{-1} a symmetric stretching mode of the central Au_3 unit plus twisting of phenyl rings presented. Au-S tangential mode on the tetramer motifs plus a rocking mode of the COOH group was found at 137.59 cm^{-1}, and an asymmetric Au-S stretching on tetramer motif coupled with a rocking mode on the phenyl ring located at 151.36 cm^{-1}. From 189.97 to 198.66 cm^{-1} Au_c-S stretching modes plus wagging mode on phenyl rings were found. The tangential mode of the S atoms forming part of the staples was found from 236.57 to 254.41 cm^{-1}. The presence of Au_c-S stretching modes coupled with rocking of phenyl rings were dispersed along the 265.63–290.89 cm^{-1} range. The Au-S stretching modes located at staples were found along the range comprised by 211.71–305.05 cm^{-1}. It is important to mention that in the range from 312.35 to 315.37 cm^{-1}, Au-S stretching modes of staples were coupled with in-plane bending modes of the phenyl rings. However, Au-S stretching modes occurring in the staples were comprised in 343.66–366.08 cm^{-1}. And the tangential S modes on the staples were spaned a range from 360.28 to 383.46 cm^{-1}. Another important vibration type is due to the chemical groups located at the tail of the ligands. For example, the stretching modes between phenyl ring and CO_2H groups are comprised in the range from 1289.16 to 1316.95 cm^{-1}, while C-C stretching modes in the phenyl ring (1342.89–1596.50 cm^{-1}), C=O stretching modes (1704.55–1794.94 cm^{-1}), C-H stretching modes (3100–3158 cm^{-1}), and O-H stretching modes (3255.01–3677.84 cm^{-1}) appears at high frequencies.

3. Conclusions

The effect of a set of six ligands on the vibrational (IR and Raman) properties of the thiolated Au_{18} cluster was carried out. It is found that the ligands effect is not necessarily related to their bulkiness, but to the presence of chemical groups able to interact among them. In such

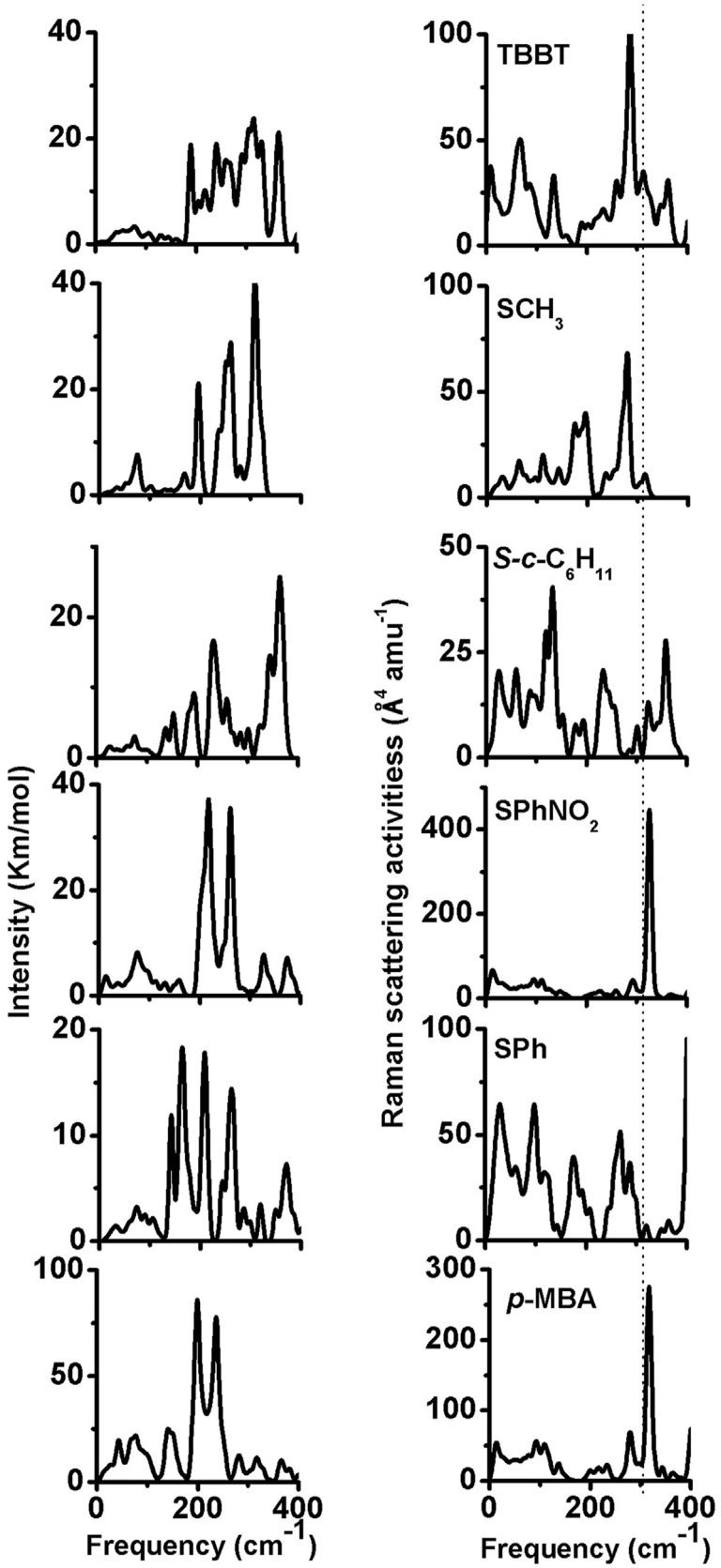

Fig. 4. Calculated IR and Raman spectra of studied compounds. Displayed spectra are based on DFT calculations. Note the difference in the intensities depending on the protecting ligands. More intense IR spectrum is due to p-MBA protected cluster while strong intensities are displayed in the Raman spectrum of $PhNO_2$ ligand. Dotted line indicates a peak located circa 300 cm^{-1} that is present in five of six spectra. A Gaussian broadening of 5 cm^{-1} is used.

manner, they might assemble or orientate forming patterns when the space on the surface of the gold core is reduced. Therefore, a strong distortion is expected to take place and IR and Raman spectra will look different than the spectra obtained by using SCH_3 ligands. Moreover, Raman spectra are found to feature characteristic peaks along all studied ligands and thereby are expected to be used as *fingerprint* of thiolated gold clusters. Finally, it was correlated the contribution of chemical groups to displayed bands on IR and Raman spectra.

Acknowledgements

The author acknowledges the support by the grant PRODEP DSA/103.5/15/6797, and thankfully acknowledge the computer resources, technical expertise and support provided by the Laboratorio Nacional de Supercómputo del Sureste de México.

Appendix A. Supplementary material

Supplementary data associated with this article can be found in the online version at http://dx.doi.org/10.1016/j.pnsc.2016.09.008.

References

[1] (a) T.G. Schaaff, G. Knight, M.N. Shafigullin, R.F. Borkman, R.L. Whetten, J. Phys. Chem. B. 102 (1998) 10643–10646;
(b) T.G. Schaaff, R.L. Whetten, J. Phys. Chem. B 104 (2000) 2630–2641.
[2] P.D. Jadzinsky, G. Calero, C.J. Ackerson, D.A. Bushnell, R.D. Kornberg, Science 318 (2007) 430–433.
[3] H. Häkkinen, M. Walter, H. Grönbeck, J. Phys. Chem. B 110 (2006) 9927.
[4] (a) M.W. Heaven, A. Dass, P.S. White, K.M. Holt, R.W. Murray, J. Am. Chem. Soc. 130 (2008) 3754;
(b) M. Zhu, C.M. Aikens, F.J. Hollander, G.C. Schatz, R. Jin, J. Am. Chem. Soc. 130 (2008) 5883;
(c) J. Akola, M. Walter, R.L. Whetten, H. Häkkinen, H. Grönbeck, J. Am. Chem. Soc. 130 (2008) 3756.
[5] A. Tlahuice-Flores, R.L. Whetten, M. Jose-Yacaman, J. Phys. Chem. C 117 (2013) 20867–20875.
[6] (a) S. Chen, S. Wang, J. Zhong, Y. Song, Jun Zhang, H. Sheng, Y. Pei, M. Zhu, Angew. Chem. Int. Ed. 54 (2015) 3145–3149;
(b) A. Das, C. Liu, H.Y. Byun, K. Nobusada, S. Zhao, N. Rosi, R. Jin, Angew. Chem. 127 (2015) 3183–3187.
[7] A. Tlahuice-Flores, M. Jose-Yacamán, R.L. Whetten, Phys. Chem. Chem. Phys. 15 (2013) 19557–19560.
[8] (a) N. Goswami, F. Lin, Y. Liu, D.T. Leong, J. Xie, Chem. Mater. 28 (2016) 4009–4016;
(b) P. Pandey, S.P. Singh, S.K. Arya, V. Gupta, M. Datta, S. Singh, B.D. Malhotra, Langmuir 23 (2007) 3333–3337;
(c) Y.-S. Chen, H. Choi, P.V. Kamat, J. Am. Chem. Soc. 135 (2013) 8822–8825.
[9] M.J. Hostetler, J.J. Stokes, R.W. Murray, Langmuir 12 (1996) 3604–3612.
[10] J. Petroski, M. Chou, C. Creutz, J. Organomet. Chem. 694 (2009) 1138–1143.
[11] R.C. Price, R.L. Whetten, J. Phys. Chem. B 110 (2006) 22166–22171.
[12] B. Varnholt, P. Oulevey, S. Luber, C. Kumara, A. Dass, T. Bürgi, J. Phys. Chem. C 118 (2014) 9604–9611.
[13] I. Dolamic, B. Varnholt, T. Bürgi, Phys. Chem. Chem. Phys. 15 (2013) 19561–19565.
[14] A. Tlahuice-Flores, Mol. Simul. 39 (2013) 428–431.
[15] a) A. Das, T. Li, G. Li, K. Nobusada, C. Zeng, N.L. Rosi, R. Jin, Nanoscale 6 (2014) 6458–6462;
b) Y. Song, S. Wang, J. Zhang, X. Kang, S. Chen, P. Li, H. Sheng, M. Zhu, J. Am. Chem. Soc. 136 (2014) 2963–2965;
c) Y. Pei, R. Pal, C. Liu, Y. Gao, Z. Zhang, X.C. Zeng, J. Am. Chem. Soc. 134 (2012) 3015–3024.
[16] S. Malola, L. Lehtovaara, S. Knoppe, K.-J. Hu, R.E. Palmer, T. Buurgi, H. Hakkinen, J. Am. Chem. Soc. 134 (2012) 19560–19563.
[17] C. Zeng, Y. Chen, C. Liu, K. Nobusada, N.L. Rosi, R. Jin, Sci. Adv. 1 (2015) e1500425.
[18] a) P.R. Nimmala, A. Dass, J. Am. Chem. Soc. 133 (2011) 9175–9177;
b) C. Zeng, H. Qian, T. Li, G. Li, N.L. Rosi, B. Yoon, R.N. Barnett, R.L. Whetten, U. Landman, R. Jin, Angew. Chem., Int. Ed. 51 (2012) 13114–13118;
c) A. Das, C. Liu, C. Zeng, G. Li, T. Li, N.L. Rosi, R. Jin, J. Phys. Chem. A 118 (2014) 8264–8269.
[19] a) P. Hohenberg, W. Kohn, Phys. Rev. 136 (1964) B864–B871;
b) W. Kohn, L.J. Sham, Phys. Rev. 140 (4A) (1965) A1133–A1138.
[20] S. Grimme, J. Comp. Chem. 27 (2006) 1787–1799.
[21] a) J.P. Perdew, J.A. Chevary, S.H. Vosko, K.A. Jackson, M.R. Pederson, D.J. Singh, Carlos Fiolhais, Phys. Rev. B 46 (1992) 6671–6687;
b) A.D. Becke, Phys. Rev. A 38 (1998) 3098–3100.
[22] P. Perdew, K. Burke, M. Ernzerhof, Phys. Rev. Lett. 77 (1996) 3865–3868.
[23] a) C.A. Jiménez-Hoyos, J.G. Benjamin, G.E. Scuseria, Phys. Chem. Chem. Phys. 10 (2008) 6621–6629;
b) J.P. Merrick, D. Moran, L. Radom, J. Phys. Chem. A 111 (2007) 11683–11700.
[24] Gaussian 09, Revision D.01, M.J. Frisch, G.W. Trucks, H.B. Schlegel, G.E. Scuseria, M.A. Robb, J.R. Cheeseman, G. Scalmani, V. Barone, B. Mennucci, G.A. Petersson, H. Nakatsuji, M. Caricato, X. Li, H.P. Hratchian, A.F. Izmaylov, J. Bloino, G. Zheng, J.L. Sonnenberg, M. Hada, M. Ehara, K. Toyota, R. Fukuda, J. Hasegawa, M. Ishida, T. Nakajima, Y. Honda, O. Kitao, H. Nakai, T. Vreven, J.A. Montgomery, Jr., J.E. Peralta, F. Ogliaro, M. Bearpark, J.J. Heyd, E. Brothers, K.N. Kudin, V.N. Staroverov, T. Keith, R. Kobayashi, J. Normand, K. Raghavachari, A. Rendell, J.C. Burant, S.S. Iyengar, J. Tomasi, M. Cossi, N. Rega, J.M. Millam, M. Klene, J.E. Knox, J.B. Cross, V. Bakken, C. Adamo, J. Jaramillo, R. Gomperts, R.E. Stratmann, O. Yazyev, A.J. Austin, R. Cammi, C. Pomelli, J.W. Ochterski, R.L. Martin, K. Morokuma, V.G. Zakrzewski, G.A. Voth, P. Salvador, J.J. Dannenberg, S. Dapprich, A.D. Daniels, O. Farkas, J.B. Foresman, J.V. Ortiz, J. Cioslowski, D.J. Fox, Gaussian, Inc,Wallingford CT, 2013.
[25] G. Li, C. Zeng, R. Jin, J. Am. Chem. Soc. 136 (2014) 673–3679.
[26] A. Das, T. Li, K. Nobusada, C. Zeng, N.L. Rosi, R. Jin, J. Am. Chem. Soc. 135 (2013) 18264–18267.
[27] M. Rambukwella, L. Sementa, G. Barcaro, A. Fortunelli, A. Dass, J. Phys. Chem. C 119 (2015) 25077–25084.
[28] C. Zeng, H. Qian, T. Li, G. Li, N. Rosi, B. Yoon, R. Whetten, U. Landman, R. Jin, Angew. Chem. Int. Ed. 51 (2012) 13114–13118.
[29] C. Zeng, T. Li, A. Das, N.L. Rosi, R. Jin, J. Am. Chem. Soc. 135 (2013) 10011–10013.
[30] C. Zeng, C. Liu, Y. Chen, N.L. Rosi, R. Jin, J. Am. Chem. Soc. 136 (2014) 11922–11925.
[31] (a) C. Zeng, Y. Chen, K. Kirschbaum, K. Appavoo, M.Y. Sfeir, R. Jin, Sci. Adv. 1 (2015) e1500045;
(b) A. Dass, S. Theivendran, P.R. Nimmala, C. Kumara, V.R. Jupally, A. Fortunelli, J. Am. Chem. Soc. 137 (2015) 4610–e1504613.
[32] Y. Chen, C. Liu, Q. Tang, C. Zeng, T. Higaki, A. Das, D. Jiang, N.L. Rosi, R. Jin, J. Am. Chem. Soc. 138 (2016) 1482–1485.
[33] C. Zeng, Y. Chen, G. Li, R. Jin, Chem. Mater. 26 (2014) 2635–2641.
[34] a) S. Chen, S. Wang, J. Zhong, Y. Song, Jun Zhang, H. Sheng, Y. Pei, M. Zhu, Angew. Chem. Int. Ed. 54 (2015) 3145–3149;
b) A. Das, C. Liu, H.Y. Byun, K. Nobusada, S. Zhao, N. Rosi, R. Jin, Angew. Chem. 127 (2015) 3183–3187.
[35] B. Molina, A. Tlahuice-Flores, Phys. Chem. Chem. Phys. 18 (2016) 1397–1403.
[36] M.O. Sinnokrot, C.D. Sherrill, J. Phys. Chem. A 108 (2004) 10200–10207.